81-1748

THE IMPROVEMENT OF AIRCRAFT SPECIFIC RANGE BY PERIODIC CONTROL

Elmer G. Gilbert*
The University of Michigan, Ann Arbor, Michigan 48109

and

Daniel T. Lyons†
TRW Inc., Redondo Beach, California 90278

Abstract

The possibility of improving aircraft cruise by periodic motion is investigated for subsonic aircraft with jet engines. A realistic point-mass model is formulated and the potential for improvement in specific range is studied using analytical and computational techniques. The methods of analysis, which are based on special classes of trajectories, give results which support those obtained previously using a less realistic energy-state model. Specifically, significant improvements are possible if a constraint is imposed on the maximum altitude. This conclusion is further substantiated by the computation of optimal periodic trajectories for a wide variety of aircraft characteristics and constraint altitudes. Conditions which favor significant improvement are: large thrust reserve at the constraint altitude, reasonably high lift-to-drag ratio, low constraint altitude, and low wing loading. The trajectory optimization algorithm, which is described in some detail, is especially efficient and may be useful in other applications.

Nomenclature

A	Amplitude of sinusoidal motion
C_{D_0}	Viscous drag coefficient
C_L	Lift coefficient
$\hat{C}_L$	Lift coefficient for maximum lift-to-drag
D, $(\bar{D})$	Aerodynamic drag, (scaled)
E, $(\bar{E})$	Energy-height, (scaled)
g	Acceleration due to gravity
G_1, G_2	$\frac{dh}{dx}$ on descent and ascent arcs of two-piece analysis
h, $(\bar{h})$	Altitude, (scaled)
h_m	Maximum altitude constraint
h_s	Scale height
$\bar{H}$	Cost integrand less $d\bar{V}/d\bar{x}$
J, $(\bar{J})$	Cost function
$\hat{J}$, $(\hat{\bar{J}})$	Augmented cost function (5.4)
k	Order of polynomial spline
K	Induced drag coefficient
K_1	Velocity scale factor
K_2	Distance scale factor
K_3	Cost scale factor
L, $(\bar{L})$	Lift, (scaled)
m, $(\bar{m})$	Vehicle mass, (scaled)
N	Number of points on a spline
S	Wing area
t, $(\bar{t})$	Time, (scaled)
T, $(\bar{T})$	Thrust, (scaled)
T_M	Maximum thrust limit
$\bar{T}^*_{ss}$	$4\delta/\sqrt{3}$, scaled optimal steady-state thrust
V, $(\bar{V})$	Velocity, (scaled)
V_E	Speed for maximum endurance
W	Vehicle weight
x, $(\bar{x})$	Range, (scaled)
$\bar{X}$	Range period (scaled)
$\bar{X}_1$	Range for minimum altitude of piecewise linear function
α	Angle of attack
β	Inverse of non-dimensional scale height
γ	Flight path angle
δ	1/2 min (D/L)
ϵ	Thrust offset angle
μ	Penalty coefficient
ρ	Atmospheric density
ρ_o	Atmospheric density at reference altitude
σ, $(\bar{\sigma})$	Thrust-specific-fuel-consumption (scaled)
τ	Time period
ω	Frequency of sinusoidal motion
ν	Velocity set

Subscripts

$(\ )_{RSS}$	Relaxed Steady State value
$(\ )_{SS}$	Steady-state value
$(\ )_i$	Denotes which linear piece: 1=descent, 2=ascent
$(\ )_o$	Reference value
$(\ )_m$	Maximum value

Superscripts

$\bar{(\ )}$	Implies scaled variable
$(\ )^*$	Implies optimum with respect to Specific Range
$(\ )'$	Implies d( )/dx
$\dot{(\ )}$	Implies d( )/dt

1. Introduction

For many years, it was generally assumed that fuel-optimal, fixed-range aircraft trajectories consist of three subarcs: an efficient powered climb, a steady-state constant-altitude cruise (assuming negligible mass change due to fuel consumption), and an efficient glide back to earth. It is known that the steady-state cruise arc is not necessarily optimal [1]. The analysis which shows this is subtle and highly dependent on the model of aircraft motion [2,3,4,5]. It is not unlikely that the three-arc trajectory is optimal for most aircraft. Even when it is not, it may give near optimal performance [6].

In [7], a different point of view [8] is taken. Cruise is modelled as an optimal periodic control problem in which conventional steady-state

This research was supported by the Air Force Office of Scientific Research, AF Systems Command, USAF, under Grant AFOSR-77-3158.

* Professor, Department of Aerospace Engineering.

† Member of Technical Staff, Defense and Space Systems Group. This work was performed while at the University of Michigan.

Copyright © American Institute of Aeronautics and Astronautics, Inc., 1981. All rights reserved.

M81-16268

cruise is compared to time-dependent periodic cruise. This allows the application of techniques from periodic control [9,10,11]. For example, the II-test [12] may be used in Speyer's example [1] to show that a steady-state cruise arc is not optimal. Using the energy-state model [13,14,15] for aircraft motion and the idea of relaxed steady-state control [8,10,11], it was shown in [7] that time-dependent periodic control gives better cruise performance for the F-4 aircraft and a class of subsonic aircraft models. Additional examples and a further discussion of relaxed steady-state cruise are given in [16]. Unfortunately, these results are inconclusive because the required "chattering" controls can only be approximated by physically realistic controls. The most interesting contribution of [7,16] is that an upper constraint on aircraft altitude increases the potential for reduced fuel consumption. With no constraint on altitude the suboptimal example in [1] shows an improvement of about .08% whereas the improvements in [7], which assume an altitude constraint, can exceed 30%.

The main objective of this paper is to show that these large improvements are possible when the energy-state model is replaced by a realistic point-mass model. First, simple analytical techniques based on special classes of periodic trajectories are introduced. Subject to certain limitations, they confirm that substantial improvements are possible when the maximum altitude is constrained. Second, optimal period trajectories are computed for a wide variety of aircraft characteristics and constraint altitudes. Although the computations are expensive and generate less insight than the analytical methods, they show conclusively that improved specific range is possible.

A crucial part of the optimization studies is a special computational technique. As Speyer [1] has discovered, conventional gradient descent algorithms applied in the space of control functions are ineffective because it is difficult to meet the periodicity conditions accurately. The approach taken here and in [17] is to specify the altitude and speed by periodic spline functions. Equations of motion are satisfied exactly without integration by solving them for the control functions in terms of the spline functions. Gradient descent occurs in the (finite-dimensional) spline spaces. Thus discretization and the imposition of the periodicity constraints is automatic. Control and altitude constraints are implemented by penalty functions. The approach has proved effective. It is believed that it will be valuable in other optimal control problems, including those which are not periodic.

The paper is arranged as follows. In Section 2, the aircraft model is developed and the periodic cruise problem is formulated. The basic assumptions include: a classical (subsonic) lift-drag model, an exponential atmosphere, constant thrust-specific fuel consumption, limits on maximum altitude and engine thrust. All aircraft satisfying these assumptions are characterized by three non-dimensional parameters. Section 3 reviews the energy-state model and gives the relaxed steady-state cruise results for the assumptions of this paper. The analytical techniques are discussed in Section 4. Using the model of Section 2, it is shown that a family of periodic trajectories may be generated by specifying the altitude of the trajectory. Two altitude functions (sinusoidal, piecewise linear) are considered and the fuel consumption for each is determined. The results are compared with those of Section 3. Section 5 describes the numerical procedure and reviews computational experience. The results of many computations are summarized in Section 6. Included are: a typical near-optimal solution, a discussion of the physical mechanisms by which improvement is obtained, and a figure giving performance improvement as a function of the three non-dimensional parameters. In addition, a few results are presented for a more realistic model of thrust specific fuel consumption. Section 7 summarizes the key results and mentions some extensions.

2. The Periodic Cruise Problem

The two-degree-of-freedom, point-mass model commonly used in aircraft performance analysis [14] is

$$\begin{aligned} m\dot{V} &= T\cos(\alpha+\varepsilon) - D(V,h,\alpha) - mg\sin\gamma, \\ mV\dot{\gamma} &= T\sin(\alpha+\varepsilon) + L(V,h,\alpha) - mg\cos\gamma, \\ \dot{h} &= V\sin\gamma,\quad \dot{x} = V\cos\gamma,\quad x(0)=0, \end{aligned} \tag{2.1}$$

where: m = aircraft mass (assumed constant), V = speed, γ = flight path angle, h = altitude, x = range, T = thrust, α = angle of attack, ε = thrust offset angle, g = acceleration due to gravity, D = drag, L = lift. Periodicity of the cruise requires a time $\tau > 0$ and

$$V(0) = V(\tau),\ \gamma(0) = \gamma(\tau),\ h(0) = h(\tau) \tag{2.2}$$

Constraints on thrust and altitude,

$$0 \le T(t) \le T_m,\ h(t) \le h_m, \tag{2.3}$$

are imposed, but it is assumed that the stall constraint (on α) and the ground constraint ($h(t) \ge 0$) are inactive. Let $\sigma(V,h,T)$ be the thrust-specific fuel consumption of the engine. Then the cost index (fuel weight/distance covered = (specific range)$^{-1}$) is

$$J = \frac{1}{x(\tau)} \int_0^\tau \sigma(V,h,T)\, T\, dt \tag{2.4}$$

The periodic cruise problem is: Minimize J with respect to the controls T and α and the period τ, subject to the constraints (2.1) - (2.3).

To simplify this problem, some familiar approximations are made: (a) $\cos(\alpha+\varepsilon) \approx 1$, $\sin(\alpha+\varepsilon) \approx 0$; (b) $L \approx \frac{1}{2}\rho(h)\, V^2 S\, C_L(\alpha)$, $D \approx \frac{1}{2}\rho(h)\, V^2 S(C_{D_0} + KC_L^2(\alpha))$ where S = surface area, $\rho(h)$ = air density; (c) $\rho(h) \approx \rho_0 \exp(h-h_0)/h_s$ where h_0 = reference altitude (arbitrary), ρ_0 = density at reference altitude, h_s = scale height of atmosphere; (d) $\sigma(V,h,T) \approx \sigma_1$ = constant. For subsonic flight with a jet engine, the approximations are reasonably accurate and capture the essential nonlinear dependencies. Approximation (d) is the least realistic, but it is in a certain sense a conservative approximation. See Section 6 for additional comment.

An equivalent normalized cruise problem of relatively simple form can be obtained with these approximations as follows. Since stall is avoided there is a one-to-one correspondence between L and α so L can replace α as a control. Also, $\cos\gamma > 0$ in cruise. Thus $dt = dx(V\cos\gamma)^{-1}$ can be used to substitute range as the independent variable. Scaled variables are introduced: $V = K_1\bar{V}$, $\gamma = \bar{\gamma}$, $h - h_m = K_2\bar{h}$, $x = K_2\bar{x}$, $x(\tau) = K_2\bar{X}$, $J = K_3\bar{J}$,

$L = mg\,\overline{L}$, $T = mg\,\overline{T}$. Setting $h_0 = h_m$ and choosing K_1, K_2, K_3 appropriately gives:

$$\overline{V}' = (\overline{V}\cos\overline{\gamma})^{-1}[\overline{T}-\overline{D}(\overline{V},\overline{h},\overline{L}) - \sin\overline{\gamma}], \tag{2.5}$$

$$\overline{\gamma}' = \overline{V}^{-1}(\overline{V}\cos\overline{\gamma})^{-1}[\overline{L} - \cos\overline{\gamma}], \tag{2.6}$$

$$\overline{h}' = \tan\overline{\gamma}, \tag{2.7}$$

$$\overline{V}(0) = \overline{V}(\overline{X}),\ \overline{\gamma}(0) = \overline{\gamma}(\overline{X}),\ \overline{h}(0) = \overline{h}(\overline{X}) \tag{2.8}$$

$$0 \leq \overline{T}(\overline{x}) \leq \overline{T}_m,\ \overline{h}(\overline{x}) \leq 0, \tag{2.9}$$

$$\overline{J} = \frac{1}{\overline{X}}\int_0^{\overline{X}}(\overline{V}\cos\overline{\gamma})^{-1}\,\overline{T}\,d\overline{x} \tag{2.10}$$

where the ' denotes differentiation with respect to $\overline{x}$ and

$$\overline{D}(\overline{V},\overline{h},\overline{L}) = \delta[\overline{V}^2 e^{-\beta\overline{h}} + \overline{V}^{-2} e^{\beta\overline{h}}\,\overline{L}^2] \tag{2.11}$$

Here δ and β are non-dimensional parameters

$$\delta = \sqrt{K\,C_{D_0}} = \tfrac{1}{2}\min\left(\tfrac{D}{L}\right), \tag{2.12}$$

$$\beta = 2m(\rho_0 S\,\hat{C}_L\,h_s)^{-1} = (gh_s)^{-1}V_E^{\,2}, \tag{2.13}$$

where $\hat{C}_L$ = lift coefficient at min (D/L) and V_E = speed for maximum endurance at the constraint altitude h_m. For low-drag aircraft $\delta < .03$. The parameter β depends primarily on wing loading and the constraint altitude (ρ_0 = density at the constraint altitude) and falls in the range $.02<\beta<.7$.

In solving the periodic cruise problem ((2.1) - (2.4) or (2.5) - (2.10)), the principal issue is whether or not the optimal cost (J^* or $\overline{J}^*$) is less than the optimal cost for steady-state cruise (J^*_{SS} or $\overline{J}^*_{SS}$). To obtain $\overline{J}^*_{SS}$ consider a general steady-state cruise: $\overline{V}(\overline{x}) \equiv \overline{V}_{SS}$, $\overline{\gamma}(\overline{x}) \equiv 0$, $\overline{h}(\overline{x}) \equiv \overline{h}_{SS} \leq 0$, $\overline{L}(\overline{x}) \equiv 1$, $\overline{T}(\overline{x}) \equiv \overline{T}_{SS} = \overline{D}(\overline{V}_{SS},\overline{h}_{SS},1)$, $0 \leq \overline{T}_{SS} \leq \overline{T}_m$, $\overline{J} = \overline{J}_{SS} = \overline{T}_{SS}\,\overline{V}_{SS}^{-1}$. The optimal steady-state cruise follows from the minimization of $\overline{J}_{SS}$ with respect to $\overline{V}_{SS}$ and $\overline{h}_{SS}$. For $\overline{T}_m > 4(3)^{-.5}\delta$ *the thrust constraint is inactive, the altitude* constraint is active; and

$$\overline{J}^*_{SS} = 4(3)^{-.75}\delta,\quad \overline{T}^*_{SS} = 4(3)^{-.5}\delta,$$
$$\overline{V}^*_{SS} = (3)^{.25},\quad \overline{h}^*_{SS} = 0 \tag{2.14}$$

If $T_m(T^*_{SS})^{-1} = \overline{T}_m(\overline{T}^*_{SS})^{-1}$, it is easy to see that $J\,(J^*_{SS})^{-1}$. *Thus it is possible to obtain the cost* ratio in the original problem (2.1) - (2.4) by computing the cost ratio in the normalized problem (2.5) - (2.10). The original problem is fully characterized by the three non-dimensional parameters: δ, β, and $T_m(T^*_{SS})^{-1}$. Hereafter it is assumed that $T_m(T^*_{SS})^{-1} \geq 1$ so that the thrust constraint is inactive in optimal steady-state cruise.

3. The Energy-State Approximation

The energy-state approximation involves two steps [13,14,15]. First, $\overline{V}$ is expressed in terms *of the energy height,*

$$E = \tfrac{1}{2}\overline{V}^2 + \overline{h}, \tag{3.1}$$

in the system (2.5) - (2.11). Second, it is assumed that $\overline{\gamma}$ and $\overline{h}$ vary slowly so that $\overline{\gamma}' = 0$ $\overline{h}' = 0$ are good approximations. This results in $\overline{\gamma} \equiv 0$, $\overline{L} \equiv 1$ and

$$\overline{E}' = \overline{T}-\overline{D}\,(\sqrt{2(\overline{E}-\overline{h})},\,\overline{h},1) = g_1(\overline{E},\overline{h},\overline{T}), \tag{3.2}$$

$$\overline{E}(0) = \overline{E}(\overline{X}) \tag{3.3}$$

$$\overline{J} = \frac{1}{\overline{X}}\int_0^{\overline{X}}\frac{\overline{T}}{\sqrt{2(\overline{E}-\overline{h})}}\,d\overline{x} = \frac{1}{\overline{X}}\int_0^{\overline{X}} g_2(\overline{E},\overline{h},\overline{T})\,d\overline{x} \tag{3.4}$$

In this system, $\overline{T}$ and $\overline{h}$ are viewed as controls which satisfy the constraints (2.9).

The optimum steady-state cruise for (3.2)-(3.4) is obtained by setting $\overline{E}' = 0$ and minimizing $\overline{J}$ with respect to $\overline{E}$ subject to $(0,\overline{J}) \in \gamma(\overline{E})$ where

$$\gamma(\overline{E}) = \{(g_1,g_2):\ 0 \leq \overline{T} \leq \overline{T}_m,\ \overline{h} \leq 0\} \tag{3.5}$$

is the velocity set corresponding to (3.2) *and* (3.4). The result is the same as in the previous section: (2.14) with $\overline{E}^* = .5(3)^{.5}$.

The relaxed steady-state (RSS) cruise is obtained by assuming that the controls chatter rapidly so that $\overline{E}$ is essentially constant. The *optimal RSS cruise is obtained by minimizing* $\overline{J}$ with respect to $\overline{E}$ subject to $(0,\overline{J}) \in$ convex hull of $\gamma(\overline{E})$. If $\gamma(\overline{E})$ is not convex, it is possible that the optimal RSS cruise will be more efficient ($\overline{J}^*_{RSS} < \overline{J}^*_{SS}$).

As Figure 1 shows, this is indeed the case. The details leading to Figure 1 are omitted since they are similar to those in [7], (where $\overline{T}_m$ is altitude dependent) and [16] (where both $\overline{T}_m$ and ρ are constant). From the form of $\overline{J}^*_{SS}$ and g_1 it is not difficult to see that $\overline{J}^*_{RSS}/\overline{J}^*_{SS}$ does not depend on δ. Large improvements correspond to large thrust reserve ($\overline{T}_m/\overline{T}^*_{SS} \gg 1$), low wing loading ($\beta \ll 1$) and low constraint altitude ($\beta \ll 1$).

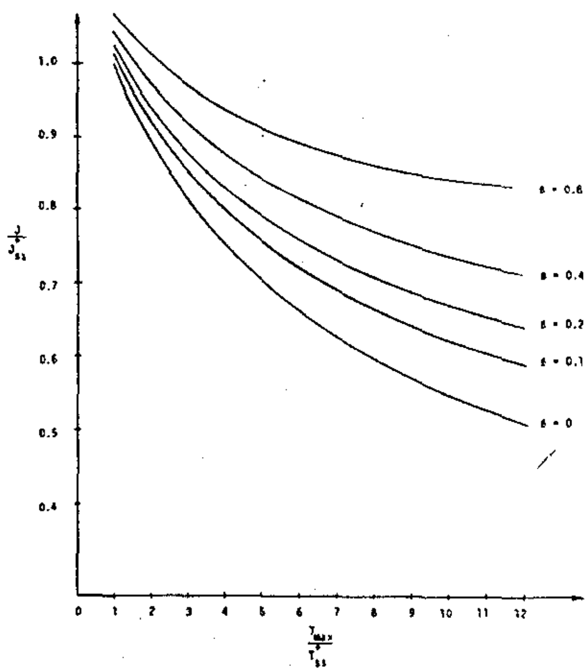

Figure 1. Cost Improvements for Relaxed Steady-State Cruise in Energy-State Model

The optimal RSS cruise is physically unrealistic and inconsistent with the assumptions of the energy-state approximation because it corresponds to jumping rapidly from flight at the constraint altitude with zero thrust to flight at a lower altitude with maximum thrust. Although the analysis is subject to question, it is encouraging and provides a simple physical explanation for improvement; thrusting is more efficient at lower altitudes where (for the same energy) speed is higher and energy addition more efficient. Since the subsequent sections utilize the point-mass model of Section 2, their results are more realistic.

4. Analysis of the Point-Mass Model

The approach of this section is to choose $\bar{h}(\bar{x})$ as a periodic function of simple form and then to optimize $\bar{J}$ with respect to the remaining functions in the system (2.5)-(2.8). The constraints (2.9) are satisfied by appropriate parameterization of $\bar{h}(\bar{x})$.

As a first step $\bar{J}$ is expressed in a different way. Solving (2.5) for $\bar{T}$ and substituting into (2.10) gives

$$\bar{J} = \frac{1}{\bar{X}} \int_0^{\bar{X}} H(\bar{V},\bar{\gamma},\bar{h},\bar{L})\, d\bar{x} \tag{4.1}$$

where

$$H(\bar{V},\bar{\gamma},\bar{h},\bar{L}) = \bar{V}^{-1}((\cos\bar{\gamma})^{-1} D(\bar{V},\bar{h},\bar{L}) + \tan\bar{\gamma}). \tag{4.2}$$

The term $\bar{V}'$ which appears in the integrand after the substitution, disappears on integration because $\bar{V}$ is periodic. Thus, the integral of $\bar{V}'$ does not appear in (4.1).

Given a periodic function $\bar{h}(\bar{x})$ the minimum of $\bar{J}$ with respect to the functions $\bar{T},\bar{L},\bar{V},\bar{\gamma}$ is obtained by the following steps:

S1. Solve (2.7) for $\bar{\gamma}$. This leads to

$$\bar{\gamma}(\bar{x}) = \tan^{-1} \bar{h}'(\bar{x}), \tag{4.3}$$

$$\cos\bar{\gamma}(\bar{x}) = (1 + \bar{h}'(\bar{x})^2)^{-.5} \tag{4.4}$$

$$\bar{\gamma}'(\bar{x}) = \bar{h}''(\bar{x})(1 + \bar{h}'(\bar{x})^2)^{-1} \tag{4.5}$$

S2. Solve (2.6) for $\bar{L}$:

$$\bar{L}(\bar{x}) = \cos\bar{\gamma}(\bar{x})(1 + \bar{V}(\bar{x})^2\, \gamma'(\bar{x})) \tag{4.6}$$

S3. Substitute (4.3),(4.4),(4.6) into (4.2). This gives H in terms of $\bar{h}(\bar{x})$ and $\bar{V}(\bar{x})$. Choose $\bar{V}(\bar{x})$ so that for each $\bar{x}$, H is minimized, i.e., $\bar{V}(\bar{x}) = \bar{V}$ where $\bar{V}$ minimizes

$$\tilde{H}(\bar{x},\bar{V}) = \bar{V}^{-1}[(\cos\bar{\gamma}(\bar{x}))^{-1} D(\bar{V},\bar{h}(\bar{x}),\ \cos\bar{\gamma}(\bar{x})\cdot (1 + \bar{V}^2\, \bar{\gamma}'(\bar{x})) + \bar{h}'(\bar{x})] \tag{4.7}$$

S4. Evaluate $\bar{J}$:

$$\bar{J} = \frac{1}{\bar{X}} \int_0^{\bar{X}} \tilde{H}(\bar{x},\bar{V}(\bar{x}))\, d\bar{x} \tag{4.8}$$

S5. Solve (2.5) for $\bar{T}$:

$$\bar{T}(x) = \cos\bar{\gamma}(x)(\bar{V}'(\bar{x})\bar{V}(x) + \bar{h}'(\bar{x})) + \bar{D}(\bar{V}(\bar{x}),\bar{h}(\bar{x}),\bar{L}(\bar{x})) \tag{4.9}$$

Because $\partial H/\partial\bar{x} = 0$ gives a quadratic equation in $\bar{V}$, $\bar{V}(\bar{x})$ is determined explicitly in S3. Steps S1 and S2 require $\bar{h}(\bar{x})$ to be twice differentiable. Since $\bar{V}'(\bar{x})$ appears in (4.9), $\bar{h}(\bar{x})$ must be three times continuously differentiable if $\bar{T}(\bar{x})$ is to be continuous. Step S5 is not necessary to evaluate the cost, but may be required to check the satisfaction of the thrust constraint (2.9). For most functions $\bar{h}(\bar{x})$, $H(\bar{x},\bar{V}(\bar{x}))$ is not an elementary function of $\bar{x}$. Thus (4.7) must be evaluated by a numerical procedure.

A simple choice for $\bar{h}(\bar{x})$ is

$$\bar{h}(\bar{x}) = A(\cos\frac{2\pi\bar{x}}{\bar{X}} - 1), \quad A \geq 0. \tag{4.10}$$

This function satisfies the altitude constraint (2.9) and is analytic so that all the functions in S1-S5 are analytic. For A=0, the steps give the optimum steady-state cruise (2.14). The integration (4.8) cannot be carried out in closed form but a very lengthy calculation shows that

$$\bar{J}(\bar{J}^*)^{-1} = 1 + \frac{\beta}{2}A + (\frac{3}{16}\beta^2 + \frac{5}{16}\omega^4 - \omega^2(\frac{\sqrt{3}}{8}\beta + \frac{1}{64}\delta^{-2} - \frac{1}{8}))A^2 + O(A^3),\ \omega = \frac{2\pi}{\bar{X}} \tag{4.11}$$

The first order term in A is positive, which means that for small A cruise performance is degraded. However, the second order term in A is negative if δ is small and $\bar{X}$ is chosen properly. Thus, if A is sufficiently large, it may be possible to improve cruise performance. For large A, the higher order terms in A may become important and the thrust constraint (2.9) may be violated.

Figure 2 summarizes the results of numerical evaluations of (4.8). Computations show that the constraint $\bar{T} \geq 0$ limits A when $T_m/T^*_{SS} > 2$. Because $\bar{J}$ is a decreasing function of A at this limit, A is determined by $\bar{T} \geq 0$. While the results in Figure 2 are not startling, they do prove that a simple periodic motion gives better performance than optimum steady-state cruise. They also give some additional information. Small values of β are desirable and the effect of δ is relatively unimportant. When the optimum period is scaled by δ it is not strongly influenced by $\beta \geq .02$. As $\beta \to 0$, the optimum period becomes large. For $\delta \leq .05$, the optimum period is large compared to the phugoid period ($\sqrt{6}\pi$) [see Figure 7].

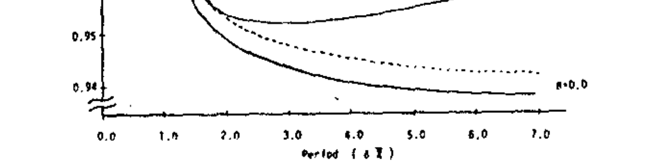

Figure 2. Cost Improvements for Sinusoidal Altitude Function (4.10). $T_m/T^*_{SS} \geq 2$.

Another choice for $\bar{h}(\bar{x})$ is the continuous piecewise linear function

$$h(x) = G_1\bar{x},\ 0\leq\bar{x}\leq\bar{X}_1 = \frac{G_2}{G_2-G_1}\,\bar{X},\ G_1 \leq 0,$$
$$= G_2(\bar{x}-\bar{X}),\ \bar{X}_1\leq\bar{x}\leq\bar{X},\quad G_2 \geq 0. \tag{4.12}$$

This function is completely determined by the period $\bar{X}$, the descent slope G_1 and the ascent slope G_2. The function can only approximate a real trajectory because it has "corners" at $\bar{x} = 0$, $\bar{X}_1$. The approximation is good if the actual trajectory which it models has smooth transitions between the constant slope segments and the period is large so that the transition phases can be neglected. This is precisely the idea used in quasi-steady-state analysis of optimal periodic control problems [8,11]. The steps S1-S5 yield rather complex formulas for the functions $\bar{V}(x)$, $\tilde{H}(x,\bar{V}(x))$, $\bar{T}(x)$, but an expression for $\bar{J}$ in terms of $\bar{X}$, G_1, G_2 can be found [18]. The results are most interesting when $\beta\bar{X}<<1$. For this situation $\bar{J}$ can be approximated more simply by assuming $\beta = 0$. This is done in what follows.

Applying S1-S5 it can be seen that $\bar{V}(\bar{x})$, $H(x,\bar{V}(x))$ and $\bar{T}(x)$ are piecewise constant functions with jump discontinuities at $x = 0, \bar{X}_1$. Let $\bar{V}_i$, $\bar{H}_i$, $\bar{T}_i$ be the constant values where $i=1$ denotes the descent interval and $i=2$ denotes the ascent interval. Then

$$\bar{V}_i = (\delta A_i)^{-.5}(1+G_i^{\,2})^{-.25}, \tag{4.13}$$
$$\bar{H}_i = \delta^{.5}(1+G_i^{\,2})^{.25}(A_i^{-.5}+G_iA_i^{.5}+\delta^2A_i^{1.5}) \tag{4.14}$$
$$\bar{T}_i = \bar{V}_i(1+G_i)^{-.5}\,\bar{H}_i \tag{4.15}$$

where
$$A_i = 2(G_i+(G_i^{\,2}+12\delta^2)^{.5})^{-1} \tag{4.16}$$

This gives

$$J = \bar{H}_1\,\frac{G_2}{G_2-G_1} + \bar{H}_2\,\frac{-G_1}{G_2-G_1} \tag{4.17}$$

Note that $\bar{X}$ does not appear in $\bar{J}$. This is a consequence of $\beta = 0$.

A simple graphical interpretation of (4.17) is given in Figure 3. The dependence of $\bar{H}_i$ on G_i has the general form indicated by the curve. For slopes G_1 and G_2, the point A has the ordinate value $\bar{J}$. Since J^*_{SS} is given by the point B (where $G_1 = G_2=0$) it is clear that $\bar{J} \leq J^*_{SS}$. The thrust $\bar{T}_i$ increases as a parameter along the curve starting at the point C where $\bar{T}_i = 0$. Thus if T_m is sufficiently large, the point E gives the lowest cost. Since $\bar{T}_i \approx 2$ implies a thrust to weight ratio of 2, the point D cannot be realized in practice and the lowest cost is obtained from a straight line which joins the point C and some point, dependent on T_m, lying between B and D. Hence the form of the best piecewise linear trajectory is a zero thrust glide followed by a maximum thrust climb. Since H_1 is minimized at $\bar{T}_1 = 0$, it follows that the glide is a maximum range glide. For small δ, $G_1 \approx -2\delta$.

The cost improvements, which can be appreciable, are summarized in Figure 4. They depend mostly on T_m/T^*_{SS} and only slightly on δ. The parameter r denotes the fraction of the trajectory spent on the downward glide. For T_m/T^*_{SS} large the glide segment is long. In general, the improvements in Figure 4 are larger than those in Figure 2. This is because the sinusoidal function (4.10) does not allow the thrust to change as rapidly between the lower and upper values as does the piecewise approximation. For $\beta = 0$, Figure 2 gives $\bar{J}/J^*_{SS} = .94$ as $\bar{X} \to \infty$. For $T_m/T^*_{SS} = 2$, which is the effective thrust reserve in Figure 2, Figure 4 gives $\bar{J}/J^*_{SS} = .91$. Thus for this rather small value of T_m/T^*_{SS} the two trajectory forms produce similar results. Based on Figures 1 and 4 one might guess that for $\beta > 0$ improvements much greater than those given in Figure 2 are possible. The best way of pursuing this conjecture is to compute optimal periodic trajectories.

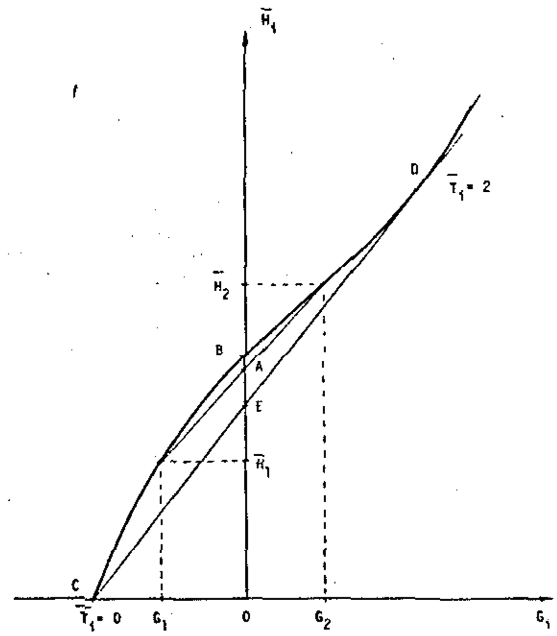

Figure 3. Graphical Interpretation of Cost for Piecewise Linear Altitude Function (4.12)

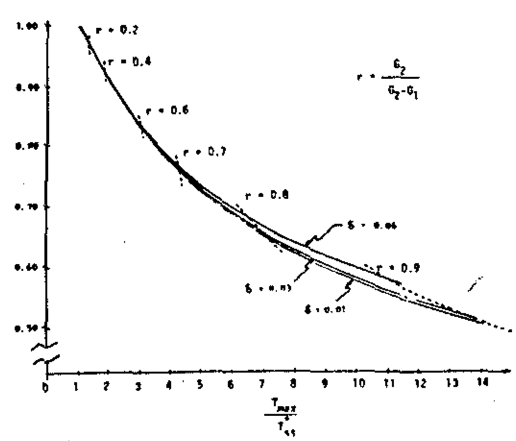

Figure 4. Cost Improvements for Piecewise Linear Altitude Function (4.12)

5. The Numerical Optimization Procedure

The class of periodic polynomial splines $f(\bar{x})$ which are used in the numerical procedure are specified by: the degree of the polynomials k, the period $\bar{X} = \bar{x}_N$ the locations of the N joints $\{0,\bar{x}_1,\ldots,\bar{x}_{N-1}\}$, and the values of f at the joints $\{f_0,f_1,\ldots,f_{N-1}\}$. More specifically, $0 = \bar{x}_0 < \bar{x}_1 \ldots < \bar{x}_{N-1} < \bar{x}_N$ and for $i = 0,\ldots,N-1$ the following conditions are satisfied:

$$f(\bar{x}_i) = f_i, \tag{5.1}$$

$$\frac{d^j f}{d\bar{x}^j}(\bar{x}_i^-) = \frac{d^j f}{d\bar{x}^j}(\bar{x}_i^+),\ j=0,\ldots,k-1 \tag{5.2}$$

$$f(\bar{x}) = p_i(\bar{x}),\ \bar{x}_i \le \bar{x} < \bar{x}_{i+1} \tag{5.3}$$

where $p_i(\bar{x})$ is a polynomial of degree k, $\bar{x}_i^+$ and $\bar{x}_i^-$ denote respectively upper and lower limits at x_i, and $\bar{x}_0^- = \bar{X}^-$. The system (5.1)-(5.3) constitutes $(k+1)N$ linear equations in the $(k+1)N$ coefficients which determine the polynomials $p_i(\bar{x})$. The system of linear equations has full rank [19] and thus $f(\bar{x})$ is uniquely determined by (5.1)-(5.3). The computation of $f(\bar{x})$ must be arranged carefully to minimize the effect of numerical errors [18]. When $f(\bar{x})$ is extended outside $[0,\bar{X}]$ by the periodicity condition $f(\bar{x}) = f(\bar{x} + \ell\bar{X})$, ℓ = integer, it is k-1 times continuously differentiable and has a piecewise constant kth derivative with jump discontinuities at the joints.

The numerical optimization procedure depends on specifying $\bar{V}(\bar{x})$ and $\bar{h}(\bar{x})$ as periodic splines, solving (2.5)-(2.8) by choice of $\bar{L}(\bar{x})$ and $\bar{T}(\bar{x})$ and evaluating (2.10) numerically. Take the joints of $\bar{V}(\bar{x})$ and $\bar{h}(\bar{x})$ to be the points of $I = \{0,x_1,\ldots,x_{N-1}\}$. The degrees of $\bar{V}(\bar{x})$ and $\bar{h}(\bar{x})$ are respectively $k_{\bar{V}}$ and $k_{\bar{h}}$. The required steps for evaluating $\bar{J}$ are:

S1. Specify $v = \{v_0,\ldots,v_{N-1}\}$ and $h = \{h_0,\ldots,h_{N-1}\}$ and determine $\bar{V}(\bar{x})$ and $\bar{h}(\bar{x})$ so that $\bar{V}(\bar{x}_i)=v_i$ and $\bar{h}(\bar{x}_i) = h_i$ for $i = 0,\ldots,N-1$.

S2. Solve (2.7) to obtain $\bar{\gamma}(\bar{x})$, $\cos\bar{\gamma}(\bar{x})$, $\bar{\gamma}'(\bar{x})$ by (4.3) - (4.5).

S3. Solve (2.6) to obtain $\bar{L}(\bar{x})$ by (4.6).

S4. Solve (2.5) to obtain $\bar{T}(\bar{x})$ by (4.9).

S5. Evaluate the integral (2.10) by numerical quadrature on the subintervals $[0,\bar{x}_1],\ldots,[\bar{x}_{N-1},\bar{X}]$ using values of the integrand on the points of $\hat{I} = \{0,\hat{x}_1,\ldots,\hat{x}_M\}$ where $0 < \hat{x}_1 < \ldots < \hat{x}_M = \bar{X}$ and I is a subset of $\hat{I}$. Denote the resulting approximation of $\bar{J}$ by $\tilde{J}(v,h)$.

Some comments are in order. The functions $\bar{h}',\bar{h}'',\bar{V}'$ are easily evaluated from the splines $\bar{h}$ and $\bar{V}$. The solution of (2.5)-(2.8) is exact. Although the functions $\bar{\gamma}(\bar{x})$, $\bar{L}(\bar{x})$, $\bar{T}(\bar{x})$ are not piecewise polynomials, they are easily evaluated on the grid $\hat{I}$ which may be taken as fine as desired. For $k_V = 1$ and $k_h = 2$, $\bar{T}$ and $\bar{L}$ are piecewise analytic with jumps possible at the points in I. For $k_V \ge k_h - 1 > 1$, $\bar{T}$ and $\bar{L}$ are (k_h-2) times continuously differentiable. Since the integrand of (2.10) is analytic on the intervals $[\bar{x}_i,\bar{x}_{i+1}]$, the error $\tilde{J}(v,h) - \bar{J}$ can be made very small (without great expense) by choosing M large. For instance, with Simpson's rule it is the order of $(\Delta\bar{x})^4$ where $\Delta\bar{x}$ bounds $|\hat{x}_{i+1}-\hat{x}_i|$, $i = 0,\ldots,M-1$.

To incorporate the constraints (2.9) a cost function

$$\hat{J}(v,h)=\tilde{J}(v,h)+\sum_{i\in I}[\mu_1 M_1(\bar{T}(\hat{x}_i))+\mu_2 M_2(h(\hat{x}_i))] \tag{5.4}$$

is introduced, where M_1 and M_2 are continuously differentiable functions which measure the constraint violations and $\mu_1,\mu_2 > 0$ are penalty coefficients. The numerical optimization is then based on an unconstrained minimization of $\hat{J}$. Since $\hat{J}$ is continuously differentiable, many efficient optimization programs are available. Because the formulas for the gradient of $\hat{J}$ are rather complex, it is convenient to choose a program which doesn't require evaluation of the gradient.

The results given in the next section were obtained under the following conditions. The grid I was uniform with M = 50. This gives an accurate evaluation of $\bar{J}$ and a detailed tabulation of the functions $\bar{\gamma}$, $\bar{T}$, $\bar{L}$. To assure a smooth trajectory and smooth controls, both $\bar{V}$ and $\bar{h}$ were cubic splines ($k_V = k_h = 3$). The functions M_1 and M_2 measured the square of the constraint violations and large values of μ_1 and μ_2 effected accurate constraint satisfaction without apparent numerical difficulties.

The optimization program was PRAXIS [20], a well developed FORTRAN subroutine not requiring derivatives. The number of function evaluations for "convergence" grows rapidly with N. To save on the number of evaluations, a two stage approach was employed: first, the trajectory was optimized for N = 6; then the resulting trajectory was used to generate an initial guess for an optimization with N = 15. Typical numbers of function evaluations were: 1000 for the first stage, 2000 for the second stage. In some cases distinct local minima were observed and several starting guesses were needed to get the best local minimum.

The grid I was nonuniform and was chosen to better represent the rapidly varying portions of the trajectory. Rather than incorporating $\bar{X}$ in the minimization process, it was optimized by interpolating optimization results for several values of $\bar{X}$. Thus, the sensitivity of the optimal cost with respect to $\bar{X}$ could be ascertained.

Note that steps S1 - S5 in Section 4 can also be used as the basis for an optimization procedure. This has the advantage that only one spline $\bar{h}(\bar{x})$ is needed. The approach has been tried and works well for $\beta > .2$. For smaller values of β the minimization algorithm was slow and erratic. Also note that the method of this section extends directly to the case where the thrust-specific fuel consumption is not constant:

$$\bar{J} = \frac{1}{\bar{X}}\int_0^{\bar{X}} (\bar{V}\cos\bar{\gamma})^{-1}\,\bar{\sigma}(\bar{V},\bar{h},\bar{T})\bar{T}\,d\bar{x} \tag{5.5}$$

The procedure of Section 4 does not work in this case because the elimination of $\bar{V}'$ from the integrand of (4.1) depends on the integrand of (2.10) being linear in T.

6. Results of Numerical Optimization

Figure 5 shows a computed solution for $T_m(T^*_{SS})^{-1} = \bar{T}_m(\bar{T}^*_{SS}) = 8$, $\delta = .0232$, $\beta = .05$. The cost ratio if $J^*(J^*_{SS})^{-1} = \bar{J}^*(\bar{J}^*_{SS})^{-1} = .743$ which represents a fuel reduction of over 25%. The included data indicate the unscaled physical units that are associated with a hypothetical aircraft having the same values of $T_m(T^*_{S})^{-1}$, δ, β. This aircraft was designed using GASP[21] and is believed to be a physically realistic aircraft. It features a high-aspect-ratio, large-area wing which produces low drag and wing loading. The minimum and maximum values of altitude and thrust are given. Note that the specified constraints on h and T are violated slightly, confirming the effectiveness of the penalty function. By chance, the minimum altitude is -187 ft., so that the ignored ground constraint is slightly exceeded.

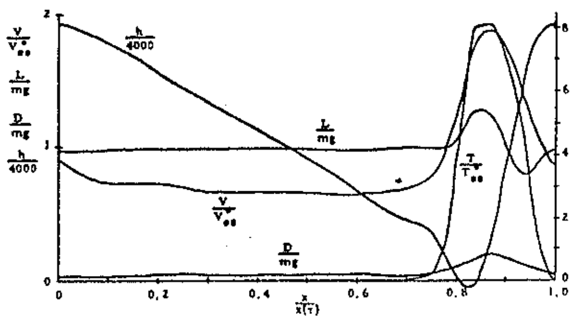

Figure 5. Optimal solution for $T_m(T^*_{SS})^{-1} = 8.$, $\beta = 0.05$, $\delta = 0.0232$. Parameters for $h_m = 7679.2$ ft., mg = 13,000 lbs., $T_m = 5572.0$ lbs., $V^*_{SS} = 289.1$ ft/sec., $x(\tau) = 194{,}000$ ft., $h_{max} = 7671$ ft., $h_{min} = -187.4$ ft., $T_{max} = 5574.6$ lbs., $T_{min} = -7.97$ lbs.

The general behavior of the optimal motions is a long, unpowered glide followed by a shorter, powered dive and climb where the speed increases rapidly and the aircraft returns to maximum altitude. Energy addition is proportional to the product of speed and thrust. Since fuel-consumption is proportional to thrust, efficiency is improved by thrusting at higher speeds. This improved efficiency more than offsets the losses associated with the powered portion of flight (increased drag from increased lift and speed). Note the powered dive just before the minimum altitude is reached. It increases the speed of the aircraft more rapidly. While the trajectory is not a "joy ride" it seems attainable: period = 36.7 miles, amplitude = 1.5 miles, normal force = $(1 \pm .25)$ mg.

Figure 6 tabulates the results of many optimizations and gives the cost ratio as a function of the three non-dimensional parameters. The cubic splines limit the cost improvement; T is continuous rather than discontinuous as necessary conditions for optimality require. Thus the cost ratios shown are somewhat greater than the theoretical best. For $\beta < .05$ the spline approximation is especially ineffective because $\bar{h}(x)$ tends to a trajectory of the form (4.12) which has corners at the points of minimum and maximum altitude. It is believed that the costs given in Figure 4 represent optimal costs as $\beta \to 0$. Thus the $\beta = 0$ cost values given in Figure 6 are those obtained from the piecewise linear altitude function.

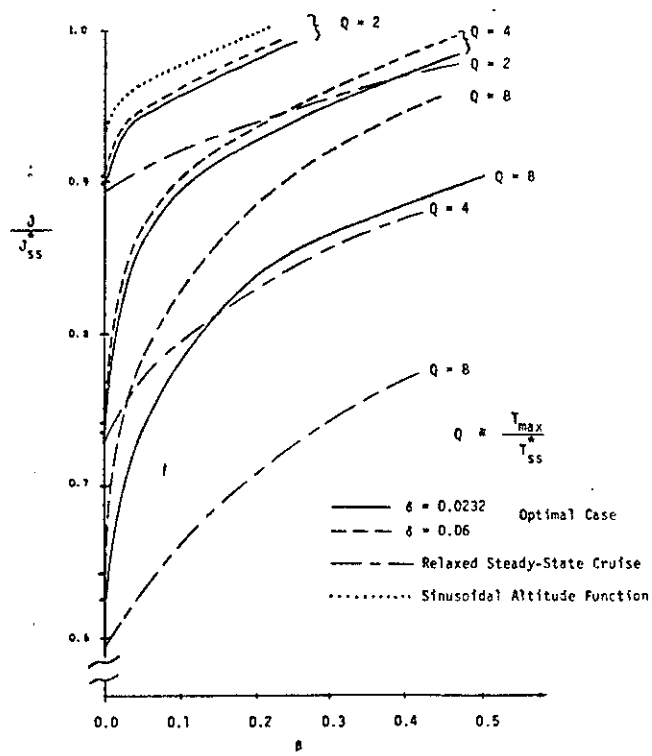

Figure 6. Computed Costs for Periodic Cruise

The results of the RSS cruise of Section 3 and the sinusoidal altitude function (4.10) are shown also in Figure 6. As might be expected, the RSS cruise results are generally better. For $\beta < .05$ they do give rough estimates of the optimal costs. The costs corresponding to the sinusoidal altitude function should be compared with the optimal costs for $T_m/T^*_{SS} = 2$. The agreement is quite good but the costs are slightly larger because of the more restricted form of the sinusoidal trajectories.

The dependence of $\bar{J}$ on the period $\bar{X}$ is shown in Figure 7. The optimal periods fall in the range obtained from the sinusoidal altitude function (4.10) and are much longer than the indicated phygoid periods. The sensitivity of $\bar{J}$ with respect to $\bar{X}$ tends to be greater for the larger values of β.

Since many modern aircraft have rather small values of δ, the critical parameters affecting improvement are β and $T_m(T^*_{SS})^{-1}$. Improvement does not occur for $T_m(T^*_{SS})^{-1} < 1$ and is slight for $T_m(T^*_{SS})^{-1} < 2$. With $\delta = .03$, $T_m = 8T^*_{SS} = .554$ mg. Thus $T_m(T^*_{SS})^{-1} = 8$ represents a large thrust ratio. The value of β is proportional to wing loading (mg/S) and inversely proportional to the air density at the constraint altitude (ρ_0). Thus, rather special aircraft, such as hypothetical aircraft described above or the U-2, are more likely to give interesting (small) values of β.

A number of optimal trajectories have been computed for a more realistic thrust-specific fuel consumption. The function $\sigma(\bar{V},\bar{h},\bar{T})$ was obtained from GASP for the hypothetical aircraft, and gives a fuel consumption which is typical of a small contemporary jet engine [18,21]. In general $\sigma(\bar{V},\bar{h},\bar{T})$ is larger at partial throttle settings than near full throttle. The main influence on the optimal trajectories is that fuel consumption is greater during the transitions between low thrust and high thrust. Thus there is a tendency toward shorter transition times, i.e., steepr dives from glide to climb. The qualitative nature of the optimal trajectories is very similar to those for constant thrust-specific fuel consumption and the optimal costs are about the same. At lower constraint altitudes steady-state cruise requires partial throttle settings where $\sigma(\bar{V},h,\bar{T})$ is large. Thus steady-state cruise is more expensive than when σ is constant. For this reason, the fractional cost improvements are greater than indicated in Figure 6. Figure 8 shows the difference in performance between the optimal steady-state cruise and the optimal periodic cruise. When σ is constant similar dependencies on the constraint altitude occur, although the differences between steady-state cruise and periodic cruise are less.

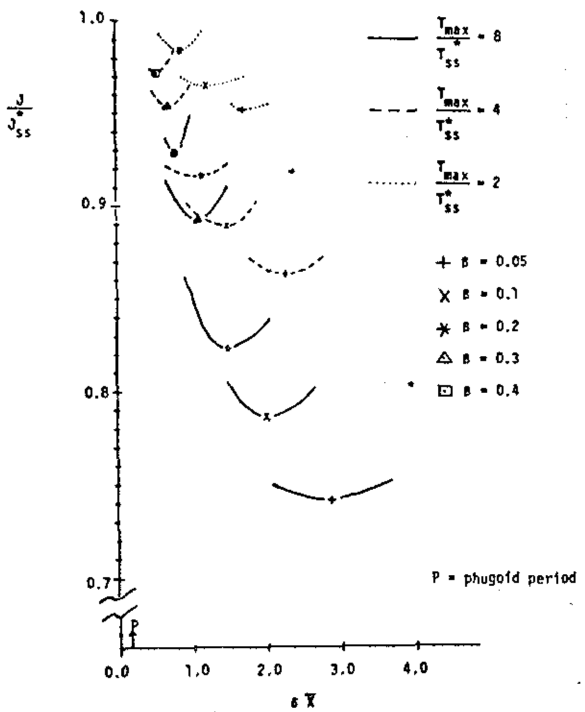

Figure 7. Dependence of Optimal Cost on Period ($\bar{X}$) for $\delta = 0.0232$

7. Conclusions

The possibility of improving aircraft specific range by periodic motion has been investigated for subsonic aircraft with jet engines. From computations based on a realistic point mass model it appears that appreciable improvements (25% or more) are possible if the maximum altitude is constrained. Several simplified methods of analysis are presented in Sections 3 and 4. They give useful information on improvement trends and lend additional insight into the mechanisms which lead to fuel reduction.

Similar methods of analysis and numerical optimization apply to the improvement of flight endurance [18]. These results will be reported in the future.

Questions concerning the computational approach remain. They include: the nature of the approximation provided by the splines, the effects of using different spline functions, methods for efficient evaluation of cost gradients, the use of gradient dependent minimization algorithms and other techniques for implementing constraints such as methods of augmented Lagrangians, and methods for treating problems in which the equations of motion cannot be solved by selecting the control functions. Such questions are presently being explored.

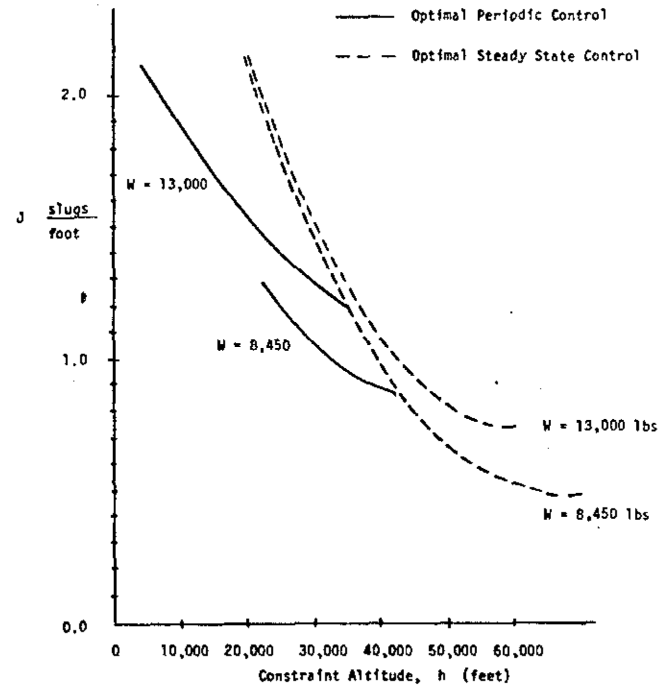

Figure 8. Range Specific Fuel Consumption for a Hypothetical Aircraft with Variable Thrust Specific Fuel Consumption

References

[1] Speyer, J. L., "Non-Optimality of Steady-State Cruise for Aircraft," AIAA Journal, Vol. 14, Nov. 1976, pp. 1604-1610.

[2] Schultz, R. L. and Zagalsky, N. R., "Aircraft Performance Optimization," J. Aircraft, Vol. 9, Feb. 1972, pp. 108-114.

[3] Schultz, R. L., "Fuel Optimality of Cruise," J. Aircraft, Vol. 11, Sept. 1974, pp. 586-587.

[4] Speyer, J. L., "On the Fuel Optimality of Cruise," J. Aircraft, Vol. 10, Dec. 1973, pp. 763-765.

[5] Zagalsky, N. R., Irons, R. P., and Schultz,R., "Energy-State Approximation and Minimum-Fuel Fixed-Range Trajectories," J. Aircraft, Vol. 8, June 1971, pp. 488-490.

[6] Erzberger, H. and Lee, H., "Constrained Optimum Trajectories with Specified Range," J. Guidance & Control, Vol. 3, Jan.-Feb. 1980, pp. 78-85.

[7] Gilbert, E. G. and Parsons, M. G., "Periodic Control and the Optimality of Aircraft Cruise," J. Aircraft, Vol. 13, Oct. 1976, pp. 828-830.

[8] Gilbert, E. G., "Vehicle Cruise: Improved Fuel Economy by Periodic Control," Automatica, Vol. 12, March 1976, pp. 159-166.

[9] Bailey, J. E., "Periodic Operation of Chemical Reactors: A Review," Chemical Engineering Communications, Vol. 1, 1973, pp. 111-124.

[10] Gilbert, E. G., "Optimal Periodic Control: A General Theory of Necessary Conditions," SIAM J. Control & Optimization, Vol. 15, Aug. 1977, pp. 717-746.

[11] Guardabassi, G., Locatelli, A., and Rinaldi, S., "Status of Periodic Optimization of Dynamical Systems," J. Optimization Theory & Applications, Vol. 14, 1974, pp. 1-20.

[12] Bernstein, D. S. and Gilbert, E. G., "Optimal Periodic Control: The π Test Revisited," IEEE Trans. Automatic Control, Vol. AC-25, Aug. 1980. pp. 673-684.

[13] Rutowski, E. S., "Energy Approach to the General Aircraft Performance Problem," J. Aeronautical Science, Vol. 21, March 1954, pp. 187-195.

[14] Bryson, A. E., Desai, M. N., and Hoffman, W. C., "Energy-State Approximation in Performance Optimization of Supersonic Aircraft," J. of Aircraft, Vol. 6, Nov.-Dec. 1979, pp. 481-488.

[15] Kelly, H. J., "Aircraft Maneuver Optimization by Reduced-Order Approximation," Controls and Dynamic Systems: Advances in Theory and Applications, C. T. Leondes (ed.), Vol. X, Academic Press, N.Y., 1973, pp. 131-178.

[16] Houlihan, S. C., Cliff, E. M. Kelly, H. J., "A Study of Chattering Cruise," AIAA/AAS Astrodynamics Conference, Danvers, Mass, Aug. 1980.

[17] Gilbert, E. G., Lyons, D. T., "Improved Aircraft Cruise by Periodic Control: The Computation of Optimal Specific Range Trajectories," Proc. 1980 Conference Information Sciences and Systems, Princeton University, Princeton, N.J., March 1980, pp. 602-607.

[18] Lyons, D. T., "Improved Aircraft Cruise by Periodic Control," Ph.D. dissertation, Dept. Aerospace Engineering, University of Michigan, 1980.

[19] de Boor, C., A Practical Guide to Splines, Springer-Verlag, N.Y., 1978.

[20] Brent, P., Algorithms for Minimization Without Derivatives, Prentice-Hall, N.Y., 1972.

[21] General Aircraft Synthesis Program, Rept. No. CR-152303, NASA-Ames Research Center, 1978.